Hydrological Sciences Journal

ISSN: 0262-6667 (Print) 2150-3435 (Online) Journal homepage: http://www.tandfonline.com/loi/thsj20

Improving global rainfall forecasting with a weather type approach in Japan

Jean-Francois Vuillaume & Srikantha Herath

To cite this article: Jean-Francois Vuillaume & Srikantha Herath (2016): Improving global rainfall forecasting with a weather type approach in Japan, Hydrological Sciences Journal, DOI: 10.1080/02626667.2016.1183165

To link to this article: http://dx.doi.org/10.1080/02626667.2016.1183165

Accepted author version posted online: 03 Jun 2016.
Published online: 09 Sep 2016.

HYDROLOGICAL SCIENCES JOURNAL – JOURNAL DES SCIENCES HYDROLOGIQUES, 2016
http://dx.doi.org/10.1080/02626667.2016.1183165

Improving global rainfall forecasting with a weather type approach in Japan

Jean-Francois Vuillaume and Srikantha Herath

Department of Global Changes and Sustainability, United Nations University Institute for the Advanced Study of Sustainability (UNU-IAS), Tokyo, Japan

ABSTRACT

An automated version of the weather type classification scheme was performed over Japan to characterize daily circulation conditions. A daily gridded field of mean sea-level pressure (MSLP) from the European Centre for Medium-Range Weather Forecasts (ECMWF) Re-Analysis dataset (ERA-interim) and the THORPEX Interactive Grand Global Ensemble (TIGGE) daily forecast dataset were used. The weather type is advantageous as it provides an opportunity to improve global rainfall prediction by refining statistical bias correction. We distinguished 11 weather types: anticyclone, cyclone, hybrid and eight purely wind directions. The results indicate that the main weather types contributing to the total volume of rainfall are cyclone, hybrid, purely westerly and northwest winds. A gamma-based bias correction decreases the global rainfall forecast root mean square by 10%, while specific weather type gamma bias correction accounts for 5–10% root mean square error reduction, with a total decrease of errors up to a maximum of 20%. Both global and weather type bias corrections improve the extreme dependency scores (EDS), but for different extreme rainfall thresholds. The study advocates the use of weather type bias-correction methods for extreme event rainfall intensity corrections higher than 100 mm/d.

ARTICLE HISTORY
Received 14 August 2015
Accepted 31 March 2016

EDITOR
A. Castellarin

ASSOCIATE EDITOR
A. Jain

KEYWORDS
weather type; bias correction; rainfall forecast; TIGGE; Japan

1 Introduction

The classification of weather patterns is an effective way of describing atmospheric circulation in a consistent manner (Rousi *et al.* 2014). It allows the definition of sub-categories of weather where patterns can be drawn. First, it accounts for the variability of the daily weather in greater detail than only considering the average temperature or rainfall of a specific location. Second, the use of automatic weather pattern classification allows the use of a computer algorithm to classify events for both forecast and climate change purposes. It then allows the use of a reasonable and manageable number of discrete classes (Huth *et al.* 2008) in comparison to the complexity of daily weather. Moreover, applications of weather typing are increasing in the areas of air quality, hydrology, forest fires, climate change variability and risks and hazards (Demuzere *et al.* 2008).

Originally, the Lamb Weather Type (LWT) classification (Lamb 1972) and the Grosswetterlagen catalogues (Hess and Brezowsky 1952) were based on pressure indices. However, subjective studies were also carried out based on circulation indices, which were initially developed for the British Isles (Jenkinson and Collison 1977, Jones *et al.* 1993). The Circulation Weather Types (CWTs) classification was carried out to identify the type of weather associated with a particular synoptic situation. A classical approach consists of computing the following indices: southerly flow (SF), westerly flow (WF), total flow (F), southerly shear vorticity (ZS), westerly shear vorticity (ZW) and total shear vorticity (Z). These indices are computed using sea-level pressure (SLP) values obtained for the 16 grid points distributed on a regular grid of 5, 6, 8 or 10 degrees. Results indicate that there is potential to improve the observation and prediction of temperature and the rainfall (Bower *et al.* 2007, Calvo *et al.* 2012, Lee and Sheridan 2012, Kenawy *et al.* 2014, Baltacı *et al.* 2015).

Weather types that occur over an area combine meteorological parameters, reflecting air mass characteristics at the surface, with synoptic conditions prevailing over an area. In general, quantitative meteorological parameters are used in the procedure, such as temperature, precipitation, relative humidity, wind velocity and sunshine duration. Most circulation weather type classifications are for a specific region; this explains the large variety of classifications that have been developed. They are typically defined for each day or group of consecutive days as a simple way to reflect the local circulation that actually occurred. Different methods exist for the classification of weather types, as shown by Huth *et al.* (2008) and Philipp *et al.* (2010). In addition, indices can be derived from mean sea-level pressure (MSLP) or geopotential height at 500 hPa; the former approach is currently most popular.

Bias correction of rainfall forecasts is necessary as intensity is underestimated by global numerical weather forecasts. Due to the limitations of current model resolution, the parameterization function is used to overcome this through modelling physically-based rainfall phenomena such as convective cells. In general, regression methods, also known as method of statistics (MOS), are used. Original work from Glahn and Lowry (1972), developed further by others, established a function to correct the

CONTACT Jean-Francois Vuillaume Vuillaume@student.unu.edu

systematic error or bias by the numerical weather prediction model. However, recent methods have mostly investigated enhancing the sharpness of ensemble forecast prediction by ensemble quantile correction (Verkade *et al.* 2013) and the ensemble method of statistics (EMOS) (Gneiting and Katzfuss 2014). In addition, operational weather centres, such as the European Centre for Medium-Range Weather Forecasts (ECMWF), do not perform post-processing bias correction; however, it is used by regional weather centres for dynamic downscaling. Indeed, underestimation of rainfall by numerical weather prediction systems is a recurrent issue. Furthermore, Bayesian model averaging (Raftery *et al.* 2005) focuses on improving the quality of ensemble forecasting with a Bayesian approach. However, the correction does not take advantage of the higher predictability of parameters compared to global rainfall, such as the MSLP.

A lot of attention has been paid to weather type (WT) classification and its occurrence, for instance, in climate studies (Riediger and Gratzki 2014), but its potential has not been investigated in numerical forecasts. In this study, 15 weather types were used, focusing on cyclone and anticyclone components within a seasonal and multi-approach model. However, the classification was not used as a driver to refine bias-correction methods by linking them with specific WT rainfall signatures. The recent release of the THORPEX Interactive Grand Global Ensemble (TIGGE) forecast dataset through THe Observing system Research and Predictability EXperiment (THORPEX) framework of the World Meteorological Organization (WMO) has made an extremely valuable dataset for forecast evaluation available. This dataset covers mid-range forecasts for up to 15 days. It is then possible to estimate the WT based on the MSLP forecast 10 days ahead and evaluate its persistence. Mean sea-level pressure exhibits the highest predictability score among the parameters in the ECMWF model (Haiden *et al.* 2014). Current ECMWF rainfall forecasts are generally reported to be accurate for up to 5–7 days and, therefore, gathering information for up to 10 days is already a challenge. Therefore, WT lead time skills show strong potential to improve extreme rainfall forecasts.

In this study, we used a WT approach of clustering the bias-corrected global rainfall forecast function. We used Japan as an example to illustrate the potential of the method. The method was validated in 10 major urban centres that are focused in the northwest of Japan: Tokyo, Yokohama, Nagoya, Saitama, Sendai, Chiba, Niigata, Hamamatsu, Funabashi and Hachioji (in order of population size). Our study specifically targeted rainfall in small and highly urbanized watersheds.

2 Data: observation, re-analysis, forecast data and observation station

Three online source datasets were investigated in this study: (1) the Automated Meteorological Data Acquisition System (AMEDAS) from the Japanese Meteorological Agency (JMA); (2) the ECMWF Re-Analysis interim (ERA-interim); and (3) the THORPEX Interactive Grand Global Ensemble (TIGGE). These are detailed below and a summary of the available period and duration of each dataset is shown in Table 1.

Table 1. Available datasets used for the study.

Dataset	Date available	Duration (in years)
ERA-interim ECMWF	1 January 1979	34
TIGGE ECMWF	2 November 2006	9
AMEDAS station	1978–2015	37

As indicated, the TIGGE ECMWF dataset covers only 9 years of forecast data. In addition, AMEDAS data available through the Japanese Meteorological Agency (JMA) provide a uniform rainfall record with an average raingauge density of 17 km and 10 min sampling over Japan. Data for the whole of Japan can be easily accessed on the internet. However, even with a high density and short time step record (10 min), the data have been recognized as insufficient to fully predict natural hazards (Shoji and Kitaura 2006) in Japan. Several stations retrieved from the AMEDAS Japan database are located in major urban cities. Table 2 summarizes the main Japanese urban centres by population size and latitude/longitude coordinates.

The locations of AMEDAS observation stations, as well as the ERA and forecast grids, are illustrated in Figure 1. The ERA-Interim dataset is the latest global atmospheric re-analysis produced by the ECMWF. It is an atmospheric model and assimilation system much improved from the ERA-40 and, therefore, ERA-Interim represents a third-generation re-analysis. ERA-Interim extends from 1979 to the present day. The key strengths of the ERA-Interim are summarized as (Dee *et al.* 2008): (a) a complete spatial and temporal dataset of multiple variables at high resolution; and (b) an improvement in low-frequency variability and stratospheric circulation. There are, however, still limitations, such as high-intensity water cycling (precipitation, evaporation) over the oceans, and positive biases in temperature and humidity below 850 hPa in the Arctic compared to radio sounding: it does not capture the low level of temperature inversion. Regarding dataset quality, Kenawy *et al.* (2014) confirmed that ERA-40 and National Centers for Environmental Prediction/National Center For Atmospheric Research (NCEP/NCAR) re-analysis gave similar results in a case study conducted over Saudi Arabia.

The TIGGE dataset provides predictions from the leading NWP centres around the globe. It is dedicated to scientific research on predictability and development of probabilistic weather forecasting methods. THORPEX is part of the World Weather Research Programme, under the auspices of the WMO Commission for Atmospheric Sciences (CAS), and is a key research component of the WMO Natural Disaster Reduction and Mitigation Programme.

Table 2. Meteorological observation stations retrieved from AMEDAS database and used in this study.

Station	Urban population	Lat., N	Long., E
Tokyo	8 637 000	35.68	139.73
Yokohama	3 631 000	35.45	139.65
Nagoya	2 239 000	35.17	136.92
Saitama	1 192 000	35.86	139.65
Sendai	1 030 000	38.25	140.89
Chiba	939 000	35.6	140.12
Niigata	813 000	37.92	139.05
Hamamatsu	534 620	34.71	137.73
Funabashi	533 270	35.69	140.02
Hachioji	507 100	35.45	139.32

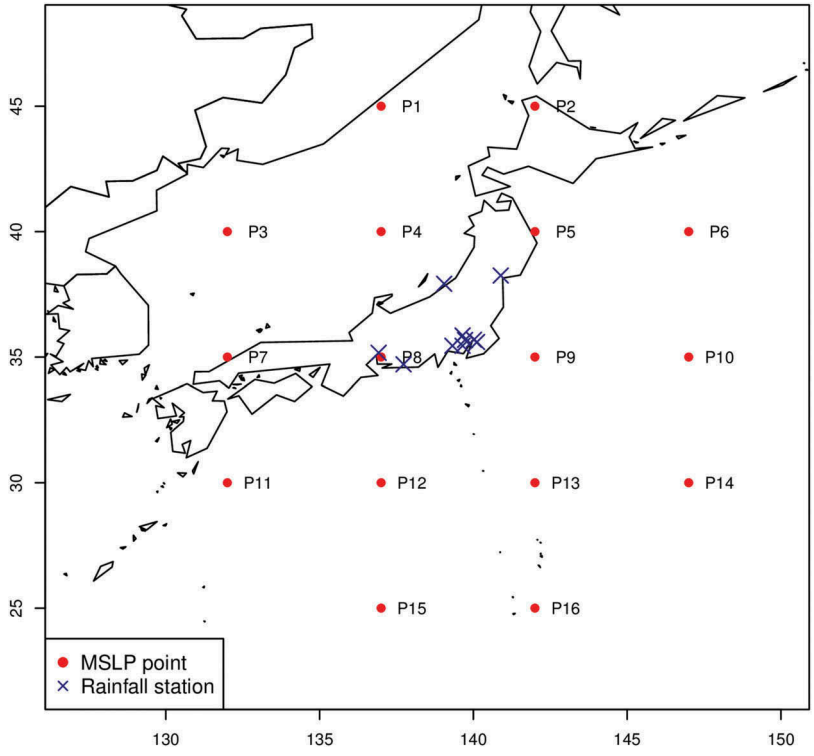

Figure 1. Pressure point locations used to compute the GLW weather classification. The grid represents an extract of the ECMWF grid onshore at 0.5° resolution. The stations used for rainfall computation (Tokyo, Yokohama, Nagoya, Saitama, Sendai, Chiba, Niigata, Hamamatsu, Funabashi and Hachioji) are indicated by crosses.

The TIGGE data provide a unique set of forecast data that can be compared and optimized in all regions of the globe (Bougeault *et al.* 2010). We used the control forecast of the Grand Ensemble rainfall computed by the ECMWF Integrated Forecast System (IFS) as it presents a larger range of the time period available (9 years) and better accuracy of the forecast products.

3 Methods

3.1 Weather type determination

The COST 733 EU project proposed the following definition for weather typing: a weather type is defined as a "*simple, discrete characterisation of the current atmospheric conditions on the nominal scale. It may include temperature, precipitation and other climate elements for characterisation*" (COST733 2015).

We used MSLP-based methods and the popular "Gross" WTs defined by the German weather agency (Deutscher Wetterdienst) and based on Lamb WTs. The classification uses six different parameters that allow the computation of the wind flow direction and the anticyclone/cyclone character of perturbation. The last weather type is labelled "hybrid cyclone" or "hybrid anticyclone", or simply "hybrid". The six parameters are defined as southerly flow (SF, Equation (1)), westerly flow (WF, Equation (2)), westerly shear vorticity (ZW, Equation (3)), southerly shear vorticity (ZS, Equation (4)), resultant flow (RF, Equation (5)) and total shear vorticity (Z, Equation (6)), and were computed as given by Trigo and DaCamara (2000):

$$\mathrm{SF} = 1.35[0.25(p_5 + 2p_9 + p_{13}) - 0.25(p_4 + 2p_8 + p_{12})] \quad (1)$$

$$\mathrm{WF} = [0.5(p_{12} + p_{13}) - 0.5(p_4 + p_5)] \quad (2)$$

$$\mathrm{ZW} = 1.12[0.5(p_{15} + p_{16}) - 0.5(p_8 + p_9)] - 0.91[0.5(p_8 + p_9) - 0.5(p_1 + p_2)] \quad (3)$$

$$\mathrm{ZS} = 0.85[0.25(p_6 + 2p_{10} + p_{14}) - 0.25(p_5 + 2p_9 + p_{13})] \quad (4)$$

$$\mathrm{RF} = \left(\mathrm{WF}^2 + \mathrm{SF}^2\right)^{0.5} \quad (5)$$

$$Z = \mathrm{ZS} + \mathrm{ZW} \quad (6)$$

where p_1, p_2, …, p_{16} represent the pressure points located on the grid (Fig. 1) numbered from top left to bottom right.

First, a grid of daily pressure points for the period 1979–2014 was defined with 5° resolution (between 132–147°E and 25–45°N) and this was computed based on the ERA-Interim data. Then, the direction of a WT—southerly, southeasterly, easterly, northeasterly, northerly, northwesterly, westerly and southwesterly (S, SE, E, NE, N, NW, W and SW) was defined.

Finally, the classification criteria were defined by the flow strength (F), vorticity (Z) and mean direction (D). Jenkinson and Collison (1977) found that simple relationships between F and Z determined whether the weather was pure Lamb directional flow (S, SE, E, NE, N, NW, W and SW), hybrid or synoptic structure (anticyclone or cyclone):

- if Abs(Z) < F, the magnitude of the total shear is lower than the resulting flow, then the weather type is purely directional. The direction of a circulation type is defined

Table 3. Summary of classification of weather types.

Weather types	Classification criteria
Purely directional (SE, E, NE, N, NW, W, SW, S)	$\|Z\| < F$
Cyclonic	$Z > 2F$, $Z > 0$
Anticyclonic	$\|Z\| > 2F$, $\|Z\| < 0$
Hybrid cyclonic, and hybrid anticyclonic	$F < \|Z\| < 2F$

by adding 180° to the value if WF is positive. A 45° segment is allocated for each direction;
- if Abs(Z) > $2F$, the weather type is either anticyclone or cyclone;
- if Abs(F) is between Abs(Z) and F, the weather type is considered to be a synoptic hybrid type.

The classification of weather types is summarized in Table 3.

3.2 Rainfall cluster evaluation

Rainfall distribution can be approximated by a gamma function defined by Equation (7). We assumed that both observed and simulated intensity distributions are well approximated by the gamma distribution, as shown by Wilks (1995), Katz (1999) and Piani *et al.* (2010). For each weather type, we estimated the shape (Equation (8)) and scale (Equation (9)) of the available rainfall time series:

$$\mathrm{pdf}(p,\alpha,\beta) = \frac{\left(x^{\alpha-1}\mathrm{e}^{-\frac{p}{\beta}}\right)}{\left(\beta^{k}\Gamma(k)\right)} \tag{7}$$

(for $p > 0$ and $\alpha, \beta > 0$)

$$\alpha = \left(\bar{p}/\sigma_p\right)^2 \tag{8}$$

$$\beta = \sigma_p/\left(\overline{p^2}\right) \tag{9}$$

The shape and scale are used to determine the bias-correction function associated with each weather type.

3.3 Bias correction

The bias-correction methods developed for weather forecasts use a regression method to reduce the error of the global rainfall forecast model. We used a cumulative probability distribution bias-correction approach as a regression method to evaluate and correct the bias. A calibration/validation approach was used in order to equally divide the available time series. For each weather type associated with a major rainfall component, the shape and scale of the distribution were estimated with a gamma function on a calibration period. Then this regression law was applied in a validation period. Finally, we estimated the root mean square error (RMSE) for the same period and compared the WT approach and a global bias correction (not considering WT). A summary of the main steps is given below:

(1) The time series is divided into calibration (2006–2011) and validation (2012–2014) sets.
(2) The scale and shape are computed for the cumulative probability distribution: calibration period for both observed and forecast data.
(3) A correction coefficient is computed between the forecast and the observation.
(4) The coefficient is applied to the validation period.
(5) The quality of correction is estimated.

4 Results and discussion

The results obtained are discussed in the four subsections below: (i) the rainfall pattern that characterized extreme rainfall and WT, (ii) the rainfall forecast skills of WT, (iii) the bias correction of WT-based forecasts and (iv) statistical analysis the WT bias-correction performance.

4.1 Weather type characteristics

The physical characteristics of the WT were investigated in terms of mean rainfall (Fig. 2), mean specific humidity (Fig. 3), mean temperature (Fig. 3) and mean average wind velocity intensity (Fig. 3). All the classifications present cyclone, hybrid and SW wind, with the largest mean intensity in terms of rainfall, humidity, temperature and wind speed. Mitigated results appeared regarding the impact of the east, southeast and anticyclone events. Comparison with the classification of the other parameters supports the WT classification of mean rainfall.

4.2 Rainfall pattern

We estimated the occurrence of the WTs over the east of Japan for the period between 1979 and 2014. The analysis of WTs over Japan and their contributions as a percentage of total rainfall volume are illustrated in Figure 2. The hybrid WT presented the highest occurrence in Japan during the period 1979–2014. However, the water volume contribution was estimated at 23% and the average number of extreme events with above 100 and 150 mm/d was two, two and one event(s) in Tokyo, Hachioji and Yokohama, respectively. The second largest WT observed was anticyclone, which was associated with about 5% of the total water contribution and does not account for extreme events. Cyclonic events presented the largest rainfall contribution (34%) for the 1979–2014 period and produced the highest rate of extreme events above the 150 mm/d threshold. Furthermore, the purely NW and westerly wind WTs were, respectively, the third or fourth main contributors of total rainfall with extreme events observed at several stations.

Figures 4 and 5 illustrate the variability of WT occurrence and its seasonal variability for the period 1979–2014. Long-term change indicates an increase in rainfall associated with cyclone and hybrid WTs, while other WTs recorded a decrease in occurrence. Seasonal variation from 1979 to 2014 did not permit establishment of a strong and persistent indicator of pattern change in the distribution of WT for the period considered.

Cyclone, hybrid, NW, SW and southerly wind WTs were the major contributors of extreme events, as illustrated in Figure 6. This observation can be confirmed from data for most of the 10 urban areas, except for Niigata and Hamamatsu stations.

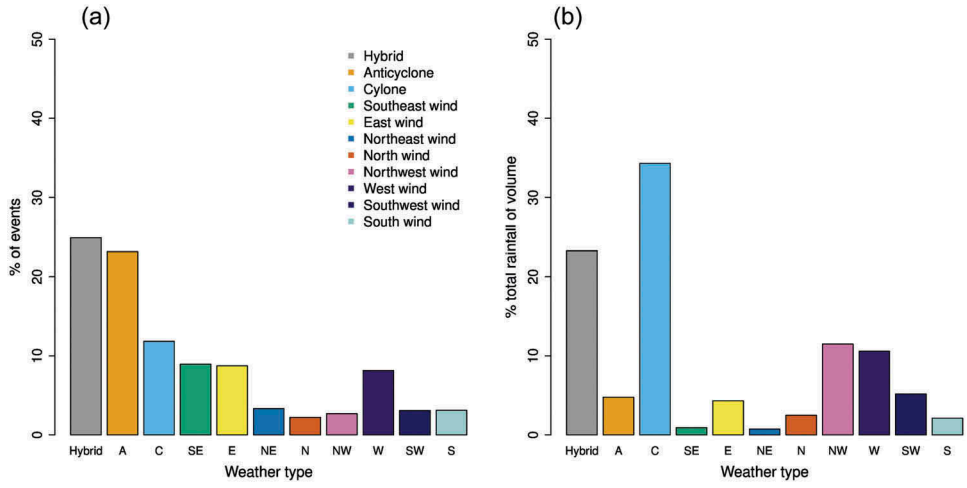

Figure 2. (a) Occurrence of weather types in Tokyo for 1979–2014. (b) Rainfall for each WT as a percentage of the total in Tokyo. Hybrid corresponds to a system with a circulation flow between purely directional flow and shear flow.

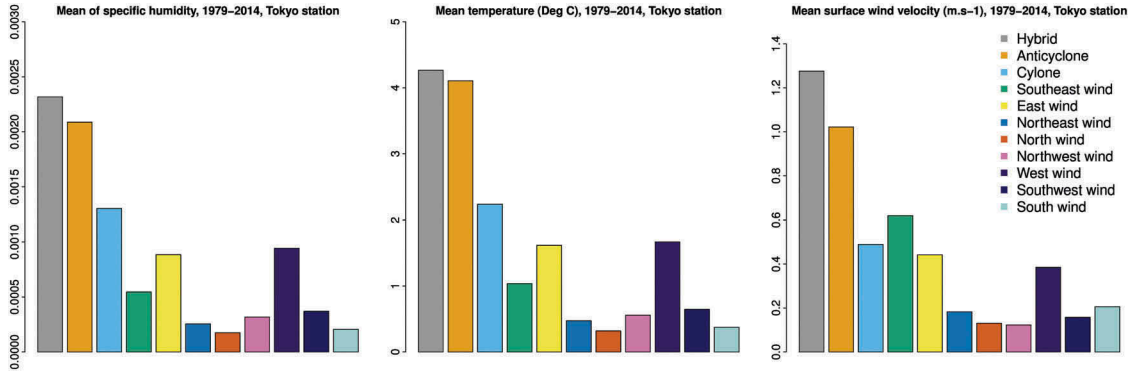

Figure 3. Weather type classification for total vertical humidity flux, temperature and wind velocity.

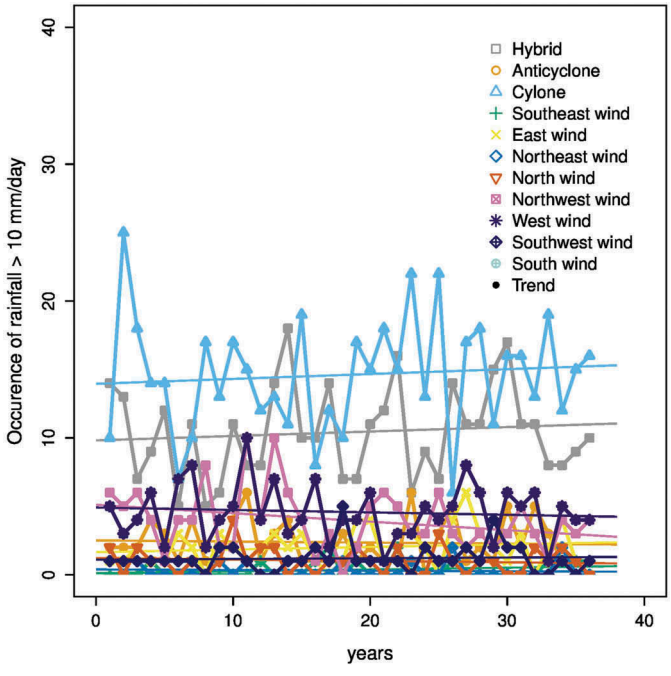

Figure 4. Annual variation of WT associated with rainfall above 10 mm/d from 1979 to 2014 and associated linear trends.

Moreover, these two locations exhibited an additional pure wind direction contribution and, therefore, were affected by their geographical location in relation to the seacoast, the central mountain chain and the regional wind patterns. Thus, Hamamatsu is exposed to easterly winds and Niigata to northerly winds, which are associated with rainfall. Nagoya presented few extreme events above 100 mm/d associated with anticyclone WT. Considering these findings, only four rainfall WT patterns were investigated:

- Hybrid
- Cyclonic
- North-westerly (NW) wind
- Westerly wind

The above four WTs produced the vast majority of extreme events in the region, with rainfall values higher than 100 and 150 mm/d. The shape *versus* scale of rainfall was computed for all 10 stations (see Table 2). The results of the analysis of the rainfall patterns are illustrated in Figure 7, which indicates the dominance of high scale numbers associated with extreme rainfall events. Hence, clusters of rainfall events are characterized by high scale and low shape numbers (Husak *et al.* 2007).

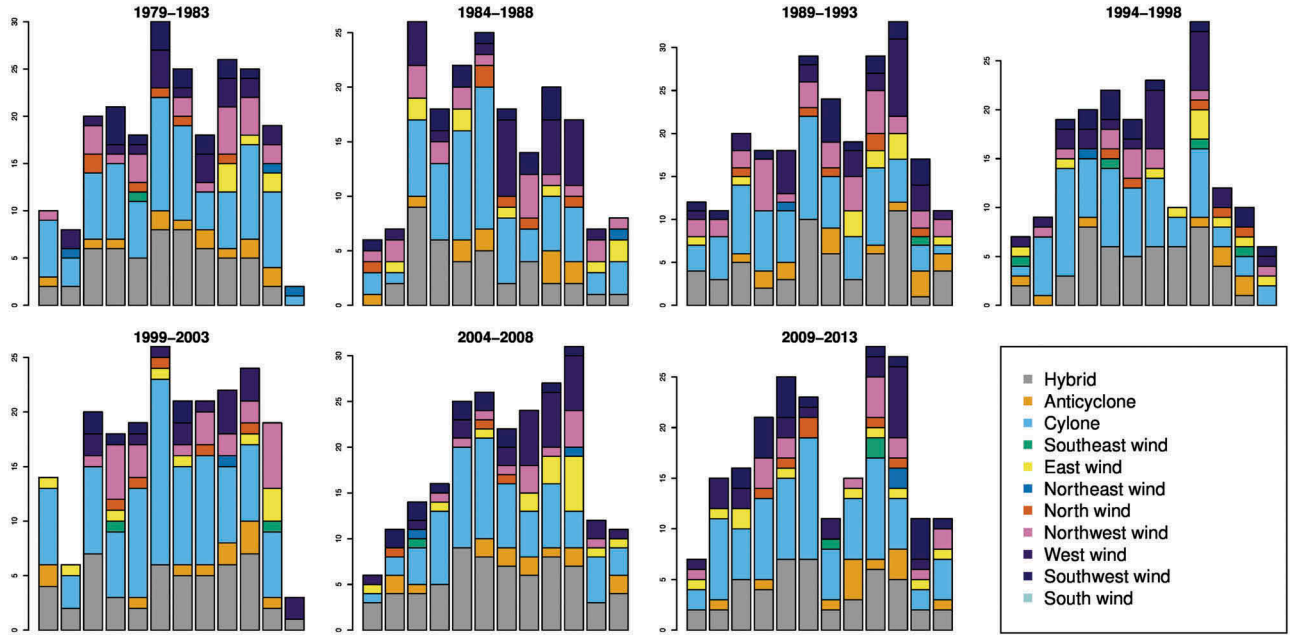

Figure 5. Five-year average seasonal variation of WTs associated with rainfall above 10 mm/d.

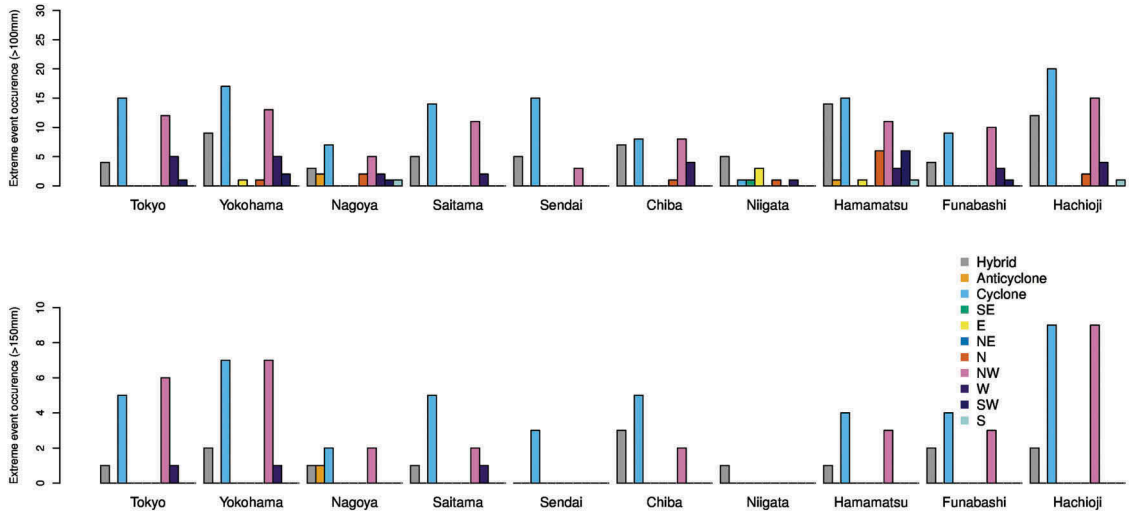

Figure 6. Occurrence of extreme event(s) for each WT at the meteorological stations located in major Japanese urban centres: (a) >100 mm/d, (b) >150 mm/d.

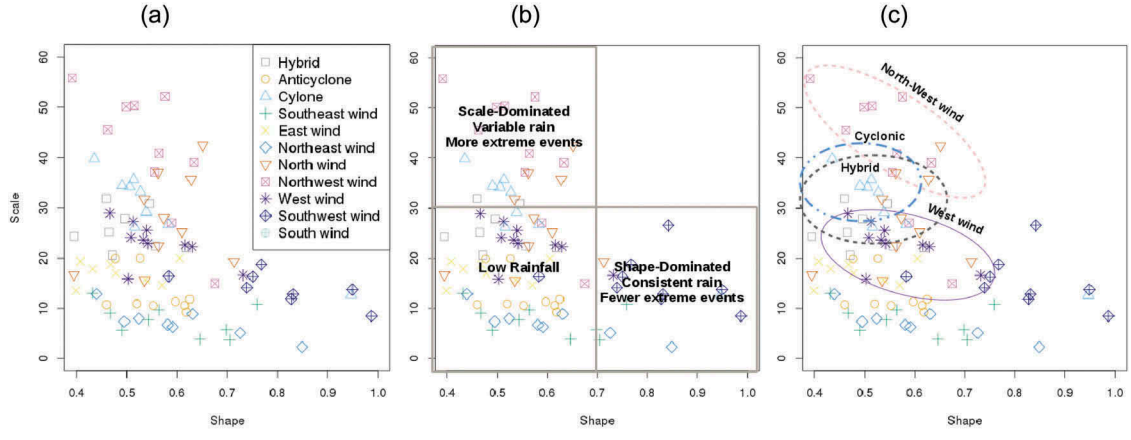

Figure 7. Cluster classification of rainfall retrieved in AMEDAS for the 10 study stations in Japan during the period 1979–2014. (a) Shape *versus* scale plot of rainfall events for each station per WT. (b) Interpretation of the rainfall type from a majority of extreme events towards fewer events. (c) Illustration of the clusters, where a cluster may enclose several cities.

4.3 Weather type forecast skills

Forecast WTs are derived from global MSLP forecasts. The MSLP is valued as the most skilful forecast parameter of global data. Therefore, WTs have the potential to improve middle-range rainfall forecasts. The performance of the WT approach is illustrated in Figure 8. Anticyclone, cyclone, purely NW wind, hybrid, purely southerly and northerly wind WTs exhibit higher predictability than randomness over a 10-day forecast. Only pure westerly wind presents low predictability and no skill after 4 days. Moreover, cyclonic, hybrid and westerly wind show predictability skills of up to 10 days. The purely NW wind has forecast skill predictability of up to 8 days. The cumulative predicted rainfall *versus* observed rainfall at Tokyo station for +24, +48, +120 and +240 h is illustrated in Figure 9. Heavy rainfall associated with cyclonic events is clearly identified on each of the forecasts. Furthermore, the extreme events associated with hybrid and westerly WTs are also identified (example of the +120 h forecast). The low predictability of the NW wind WT can be observed through the low number for this WT on each chart. The number of rainfall events without an associated WT (black dot) increases from +24 h to +240 h forecasts, illustrating the reduction in skill of WTs with increasing lead time. Therefore, the number of misses and false negative forecasts

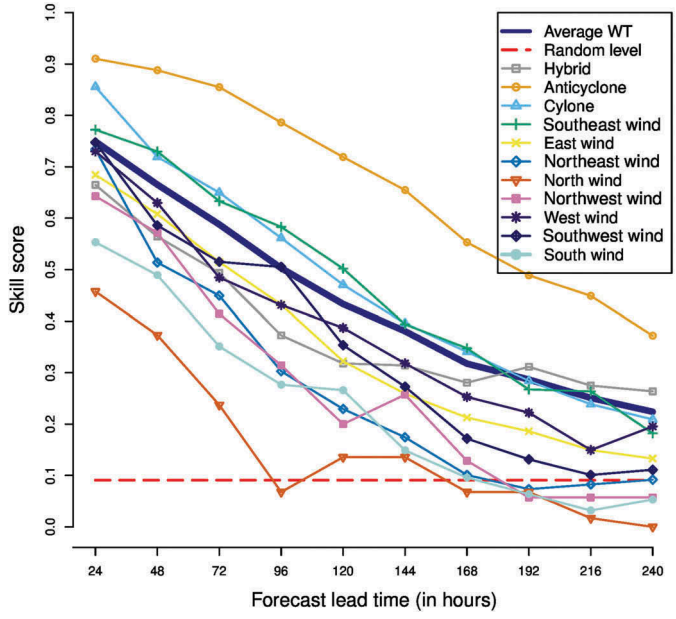

Figure 8. Skill scores of weather forecasts up to 10 days. The skill score is given from 0 to 1, where 1 indicates a perfect WT forecast, and a score <0.09 indicates no prediction skill.

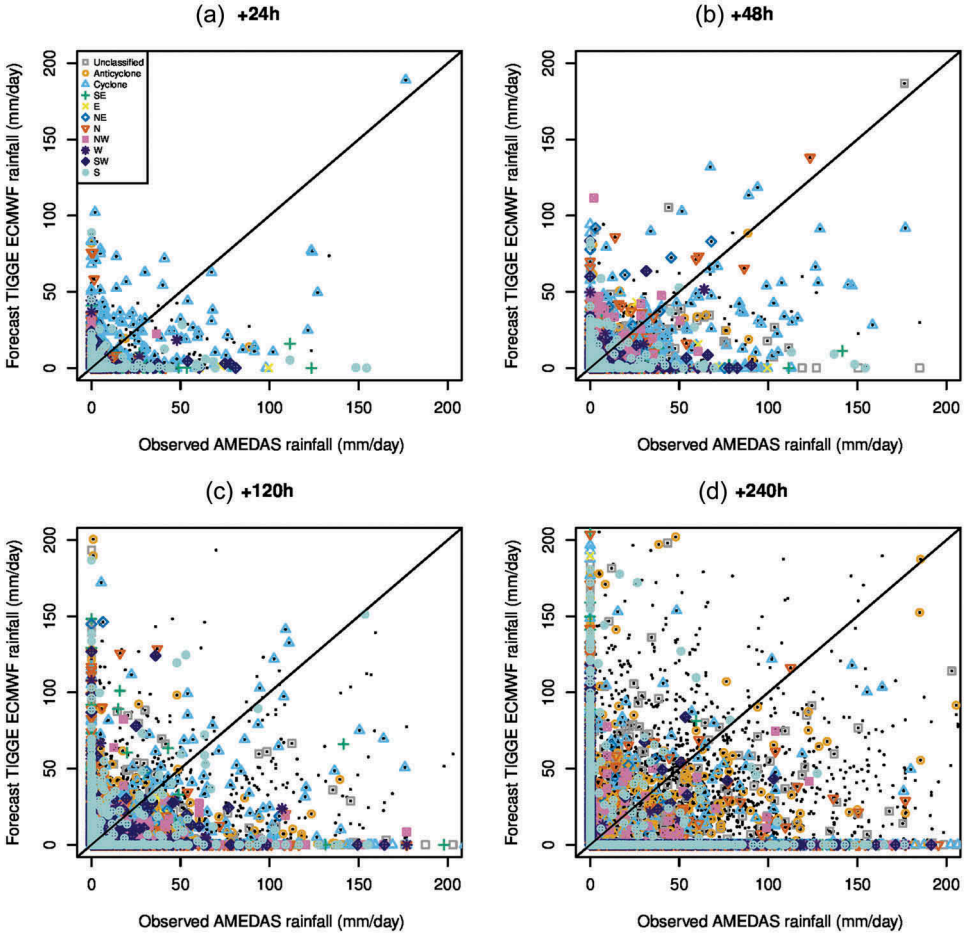

Figure 9. Tokyo observations versus raw (i.e. not corrected) +24 h, +48 h, +120 h and +240 h forecasts for all weather types for the period 2006–2014. Note that the dot without any symbol represents a missed WT forecast. The symbols localized at 0 on the *x*-axis and *y*-axis are missed forecasts or false alarms.

increases. This appears on both the vertical and horizontal axes on Figure 9 and increases with lead time.

4.4 Bias correction of forecast

A regression function based on cumulative probability distribution correction was used to forecast rainfall at 24, 48, 120 and 240 h lead times. Figure 10 illustrates the correction for the 24 h global rainfall forecast. It highlights the underestimation bias of the model. The bias of the model limits the prediction of rainfall, particularly for intensity higher than 100 mm/d. The lower performance of extreme rainfall prediction typically above 100 mm/d is indicated by the absence of the yellow dot above this threshold. The correction is particularly efficient for intensity over 100 mm/d. Then, corrected rainfall covers the whole range of intensity up to 160 mm/d instead of 90 mm/d for the raw forecast.

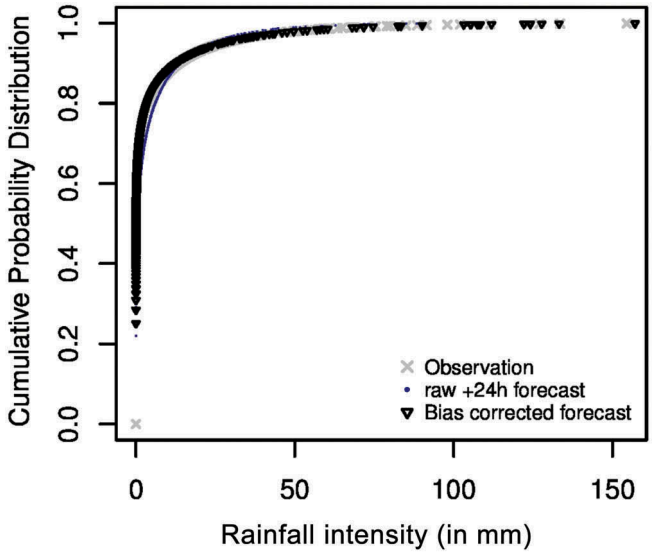

Figure 10. Rainfall cumulative distribution corrections for observations and +24 h forecast at the Tokyo station. The AMEDAS observed rainfall is represented by the grey crosses. The dotted curve indicates the original TIGGE forecast and the black triangles mark the corrected cumulative rainfall function.

Figure 11 illustrates the regression function computed for the 24, 48, 120 and 240 h ahead forecasts at the Tokyo station. For each forecast, the correction without WT is illustrated (black dot), as well as for the WTs: hybrid, cyclone, anticyclone and the eight pure wind directions. Rainfall bias correction can diverge by WT and by lead time.

Moreover, according to the results, which confirmed what previous studies had found, rainfall numerical weather forecasts indicate the need for positive bias correction. Moreover, the cyclonic and hybrid WTs diverge slightly from the global bias correction. This confirms earlier results (shown in Fig. 3), which highlighted hybrid and cyclone WTs as the main contributors of extreme rainfall. However, the 240 h lead-time global forecast illustrates the largest difference between the global correction and cyclonic WT correction. A similar case occurs for the hybrid WT at 48 and 120 h lead-time forecasts.

The purely NW wind WT presents a pattern of large divergence compared to the global bias correction, this difference decreases from short-term forecasts (+24 h, +48 h) to mid-term (+240 h), mainly due to the use of cumulative rainfall, which tends to decrease the effect of high intensity error in the forecast. The pure NW wind WT presents a more complex bias correction with a larger variability pattern than

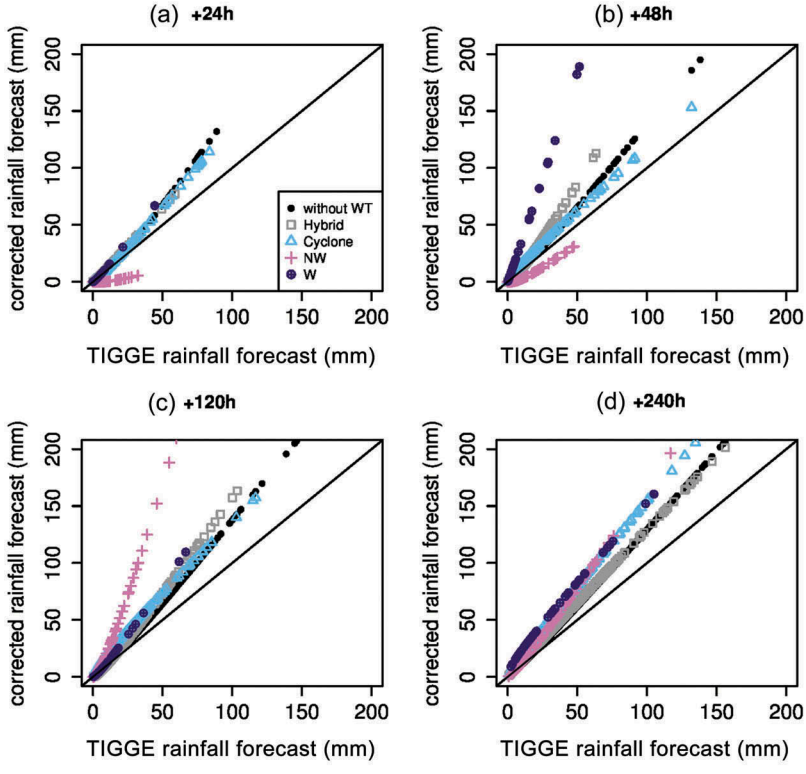

Figure 11. Bias correction model for each WT in Tokyo from 2006 to 2014: ECMWF raw rainfall forecast at +24 h, +48 h, +120 h and +240 h *versus* observations. The black line represents the correction function without WT.

other WTs. Therefore, from an overestimation of rainfall patterns for +24 h and +48 h, it becomes null for the cumulative +120 h before being aligned with the global WT line. The westerly wind WT correction curve is aligned with the NW wind for +24 h and +120 h. It becomes a null correction for the +240 h forecast. The purely westerly wind WT presents a similar pattern to that observed for the NW wind bias correction function. However, it diverges for +48 h and +240 h. This observation is interpreted by the fact that purely westerly and NW winds share common characteristics.

The results of the bias correction at the Tokyo station for different WTs, at +24 h forecast, are illustrated in Figure 12, which highlights the performance of the bias correction while not considering the differences between WTs. Figures 12(b), (c) and (d) present the result of the correction of the forecast at the Tokyo station for the hybrid WT, while Figure 12(a) shows the performance of the global bias correction (without WT). As illustrated, the hybrid type and both purely westerly and NW wind WTs show lower records than the cyclonic WT. Therefore, cyclonic WT bias correction shows similarity with the global approach. However, an improvement between cyclonic WT and the global bias correction can be observed, since several points are better located along the 45° line of perfect forecasts.

It is important to notice that the correction can become weak due to the low number of extreme events available during the 2006–2010 calibration period. Furthermore, when WTs are identified as false negative (the type is not observed, but forecast) or missed (observed WT that is not forecast), it cannot be corrected with this method. Only false rainfall intensities can be correct based on statistical laws, which are a "sub-group" of missed and false negative forecasts.

In summary, the bias correction based on hybrid automatic threshold classification allows refinement of the bias correction function. Figure 13 illustrates the divergence of the WT correction and lead time. Only a few WTs are related to extreme events and, therefore, the forecast puts more emphasis on WTs that underperform in their predictions, such as the purely westerly wind pattern. The westerly pattern affecting a few urban areas such as Hamamatsu, Hachioji, Yokohama and Nagoya does not present sufficient predictability skills.

The 24 h lead-time forecast bias correction presented in Figure 12 was expanded to 48, 120 and 240 h forecast lead times, as illustrated in Figure 13. The cumulative rainfall observed against the forecast rainfall was plotted. We can see the performance of the correction in several of the plots that show the raw (i.e. not corrected) TIGGE rainfall intensity being corrected against observed AMEDAS rainfall. Therefore, we computed the RMSE between observations and forecasts. Both hybrid and cyclone bias correction present an improvement in rainfall forecast. However, it seems that low rainfall tends to be overestimated in the case of the +240 h cyclonic WT, even when it has been relatively well corrected (most of the corrected cyclone rainfall is located above the 45°line for 240 h lead-time cyclonic WT forecast).

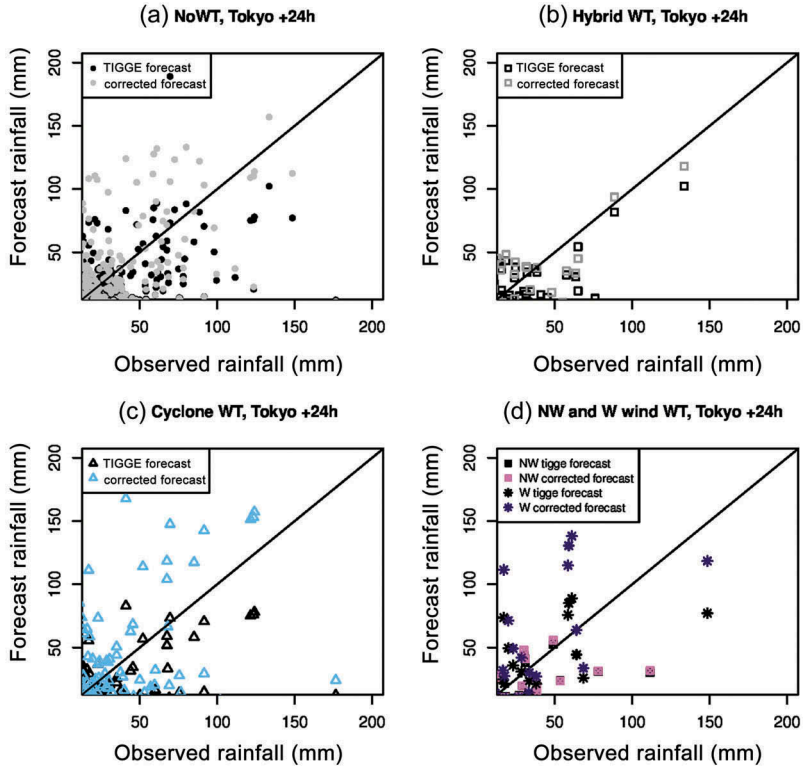

Figure 12. Corrected +24 h rainfall forecast for the three main extreme events: (a) global bias correction; (b) hybrid, (c) cyclone and (d) purely westerly and NW wind WTs. The 45° line indicates a perfect match between observed AMEDAS rainfall and ECMWF control forecast data.

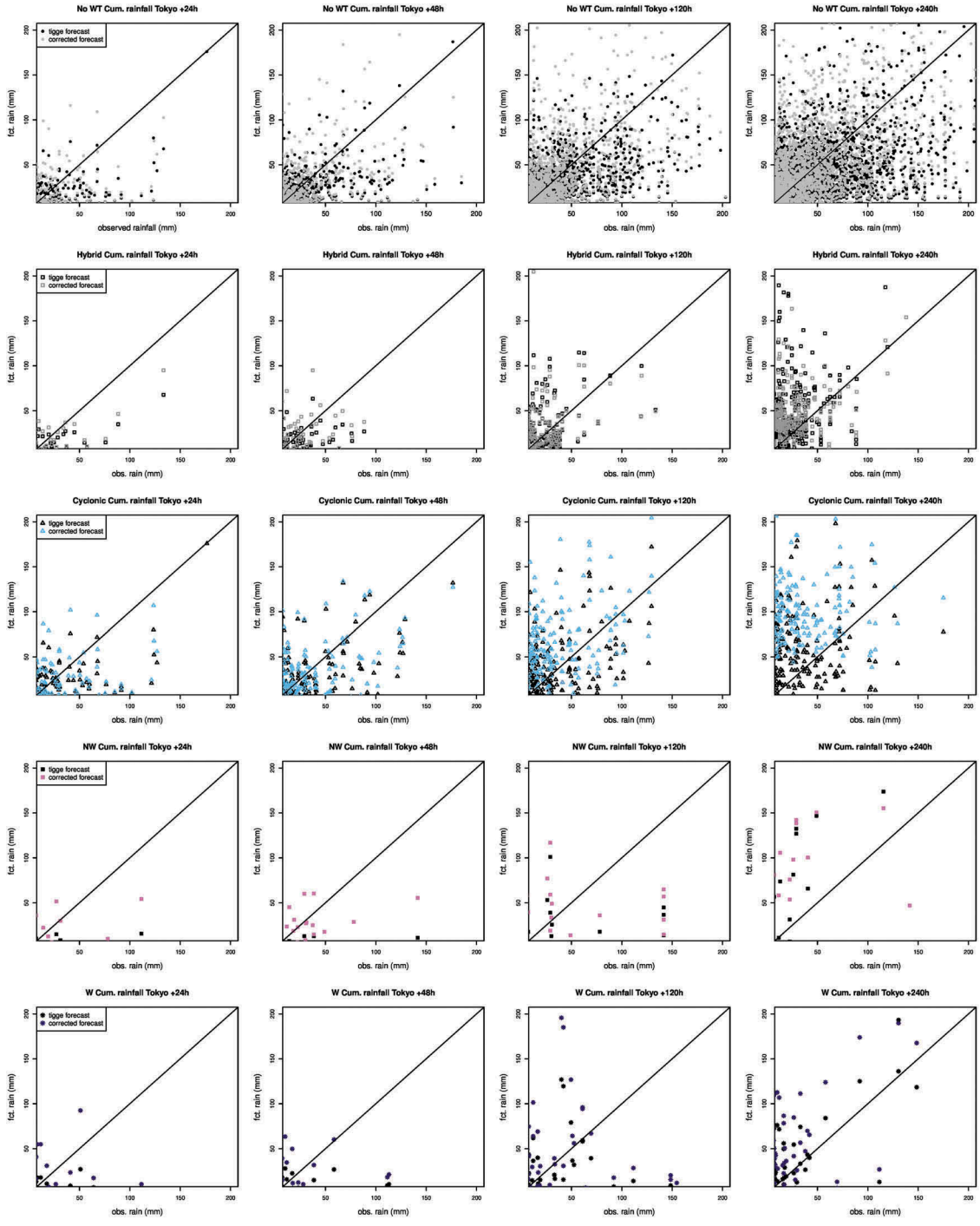

Figure 13. Performance of the bias correction for the cumulative rainfall at +24 h, +48 h, +120 h and +240 h forecast *versus* observation. A filter is applied to remove low rainfall events.

The low performance of the bias-correction model is clear in the case of +120 h purely westerly wind WT. The error is mainly due to the small number of extreme events with low forecast skill. A negative bias correction was obtained for purely westerly wind WT and +240 h lead time. This reflects the general overestimation of the purely westerly wind WT at +240 h lead-time forecast. To quantify the results, a statistical analysis based on 10 weather stations was performed, the results are presented and discussed in the following section.

4.5 Statistical analysis

Figure 14 illustrates the statistical performance of the bias correction based on WT for +24 h forecasts. The RMSE, mean average error (MAE) and change in correlation factors are estimated for three rainfall threshold values, 10, 50 and 100 mm/d, to account specifically for extreme rainfall. The results exhibit a general improvement of all WTs at each rainfall threshold, but within a broad range of performance. Moreover, WTs performed better overall than global bias

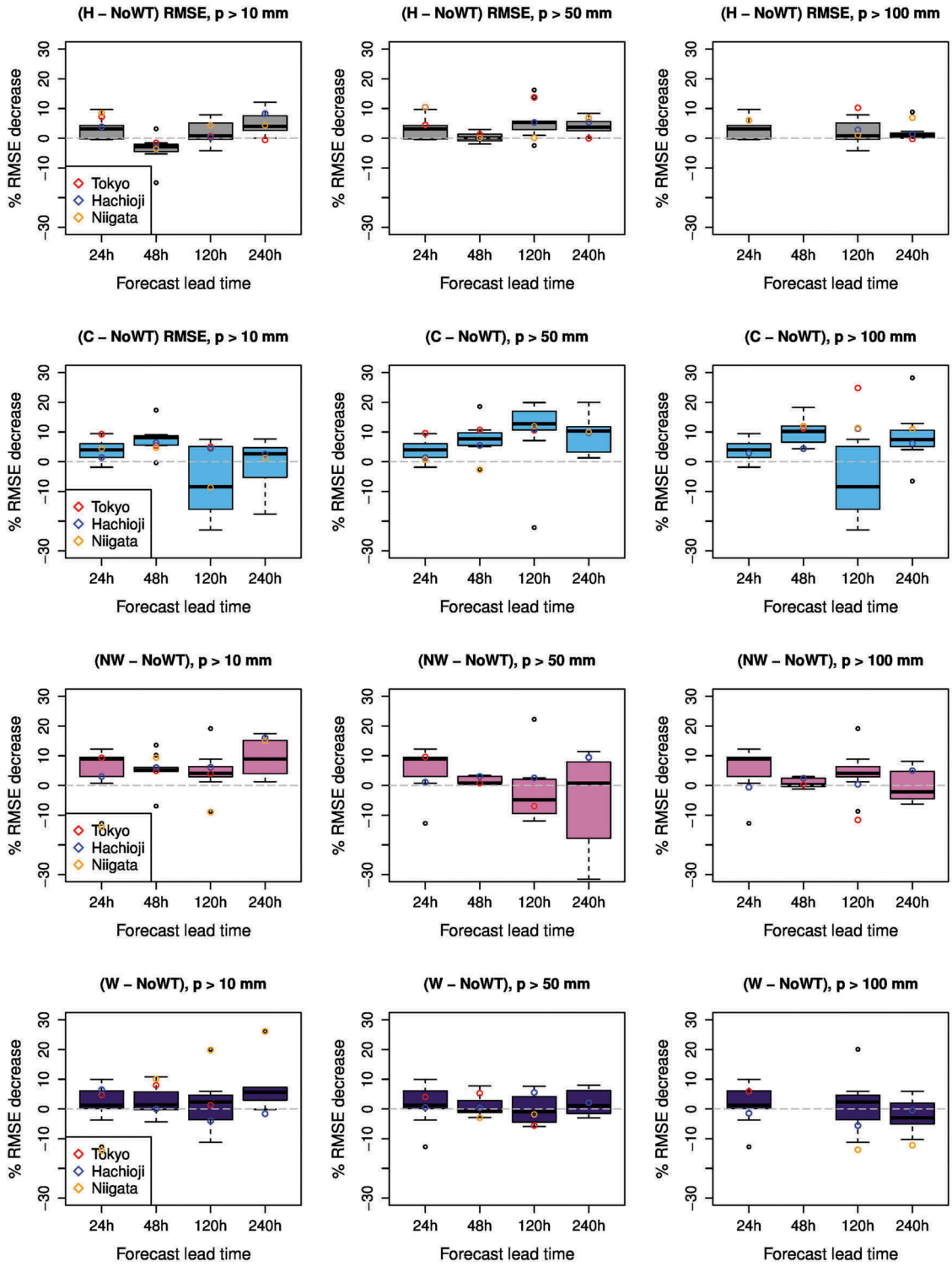

Figure 14. Box-and-whisker plots showing statistical performance of the bias correction for +48 h, +120 h and +240 h rainfall for thresholds of 10, 50 and 100 mm/d. Performance is evaluated in terms of RMSE reduction for each WT: hybrid, cyclone, NW and westerly wind. The horizontal black line in the box represents the median of the distribution (50% of the data are greater than this value), the upper and lower box limits represent the upper and lower quartiles (25% of data greater value). Maximum and minimum greatest and least values are indicated by the top and bottom horizontal lines. The outlier points indicate a value of more than two-thirds of the upper quantile.

correction (box plots are above the dashed white abscissa line). The quality increases with the rainfall intensity threshold; however, the variability of the results also increases with the rainfall. Thus, cyclonic event and NW wind WTs present an increase in performance of 0–30% and 5–25%, respectively, at the 100 mm/d threshold.

It is clear that hybrid, cyclonic and pure NW wind WTs show more improvement than the global bias correction.

However, the pure westerly wind WT shows worse performance than the global bias correction for the thresholds of 50 and 100 mm/d. The performance of the rainfall correction depends on the location of the station and it shows large variations for the cyclonic and purely NW wind WTs when rainfall is higher than 100 mm/d. The results are poor for this WT and extreme rainfall, due to the low number of purely westerly wind extreme events during the period 2006–2014. The correlation factor decreases in quality after bias correction with a large variation in the performance function of the WT and the rainfall threshold amount stations.

The skill scores of forecasts are useful tools to evaluate performance. The extreme dependency score (EDS) is used to evaluate the performance of forecast system models for rare extreme events, as defined by (Coles *et al.* 1999):

$$\mathrm{EDS} = \frac{\log\left(\frac{a+c}{n}\right)}{\log\frac{a}{n}} - 1 \tag{10}$$

where a is the hit rate, c the number of misses and n the number of events.

The EDS has the advantage of low sensitivity to rainfall threshold when contingency tables are computed (Primo and Ghelli 2009). It can be used to evaluate the quality of post-processing methods to improve rainfall forecast estimation.

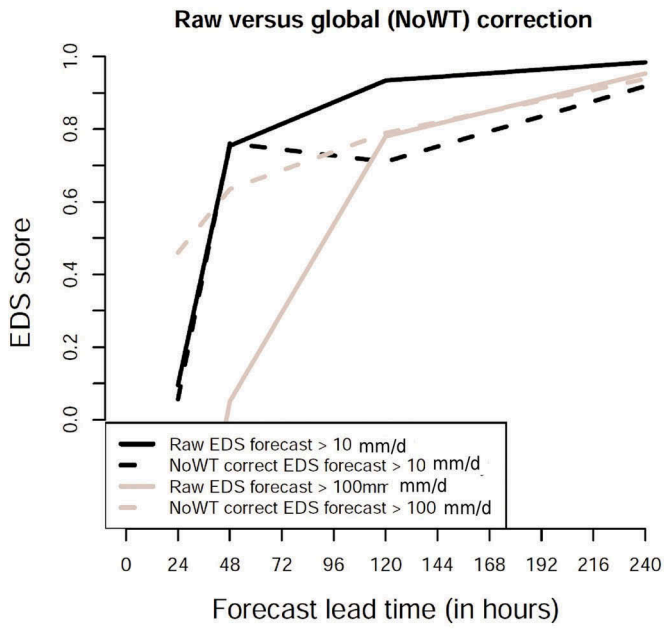

Figure 15. Extreme dependency score for raw and global corrected (NoWT) forecasts for Tokyo station with thresholds of 10 and 100 mm/d, respectively. The global observed EDS (NoWT) are indicated by solid black and grey lines for thresholds of 10 and 100 mm/d, respectively. The corrected forecast that does not use the WT approach shown by the dotted line.

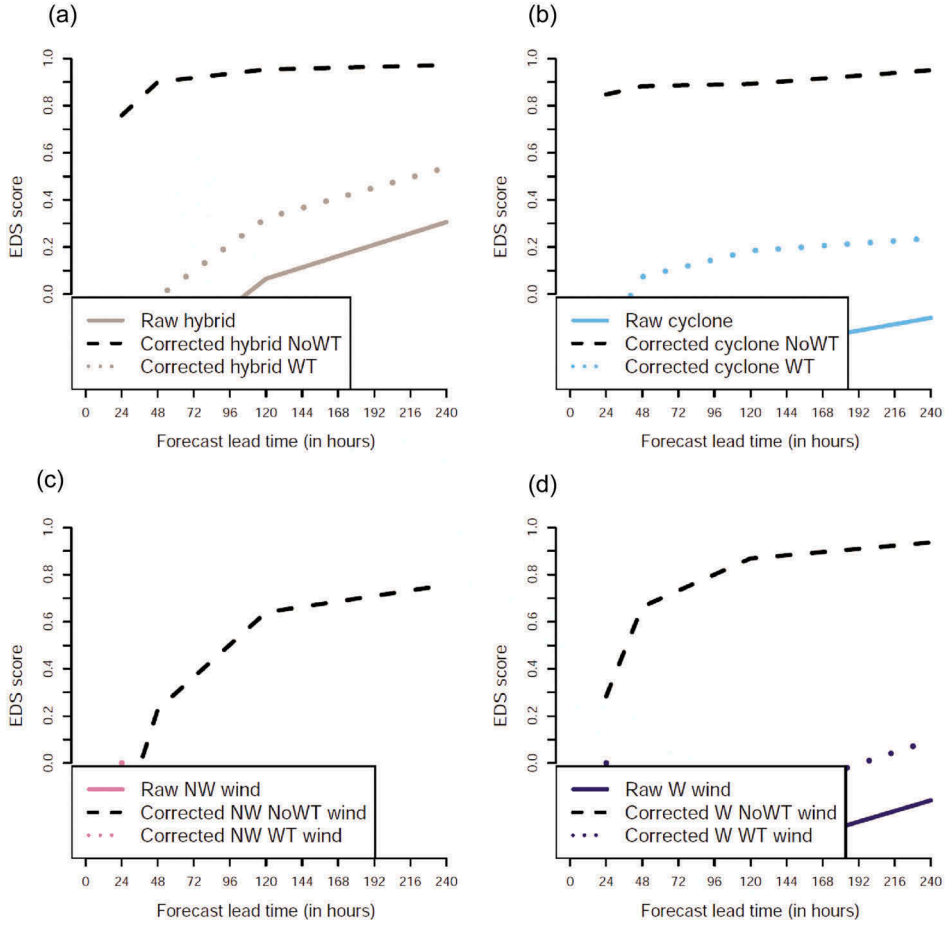

Figure 16. Extreme dependency plot per weather type for Tokyo station with a threshold of 10 mm/d. (a)–(d) Performance of individual hybrid, cyclone, NW and W wind WTs, respectively. The corrected global EDS (NoWT) is indicated by the dashed black line. The solid grey, blue, violet and pink solid lines indicate the observed EDS scores for the hybrid, cyclone, NE and W WTs. The coloured dotted lines highlight the performance of the specific WT bias correction for a rainfall threshold of 10 mm/d.

Figure 15 illustrates the EDS *versus* forecast lead time for raw (i.e. not corrected) and corrected forecasts in the case of the WT approach and the no WT (NoWT) approach. The EDS score confirms the better performance of bias correction per WT than the global approach in addition to the gain in lead time skill. For instance, the correction performed using the WT approach improves the correction compared to a global correction method.

Figures 16 and 17 illustrate the statistical performance of the weather type based bias correction for +24, +48, +120 and +240 h forecast with EDS performance for rainfall threshold of 10 and 100 mm/d. As illustrated by Figure 16, the low rainfall intensities (>10mm/d) show that the global correction (without WT approach) always performed better than the weather type approach. However as illustrated in Figure 17, for heavy rainfall (p > 100mm/d), the weather type improve the bias correction for the lead time +48, +120 and +240 h. Strong improvement can be noticed for both Hybrid and Cyclone, Figure 17(a) and Figure 17(b), respectively. Moderate improvement of EDS for Westerly wind Figure 17 (d) and small improvement for North-Westerly wind, Figure 17(d). These results confirmed and refined the results obtained in the beginning of the statistical analysis part.

5 Conclusions

In this study, we (1) determined the occurrence of weather types (WT) and their predictability skill for up to 10 days ahead in Japan, (2) assessed the rainfall characteristic of WTs and their associated extreme rainfall, and (3) attempted to improve rainfall forecast by WT clustering bias correction. The analysis presented here links the WT forecast and the bias correction. It can be applied to extreme rainfall events that occur in urban areas prone to flooding. Our findings show that the highest predictability of WTs ranges from anticyclone, hybrid, cyclone, SE, westerly, easterly, SW, NE, NW, southerly to northerly wind. However, only cyclonic, hybrid, NW and westerly wind WTs are associated with extreme events, and this is validated from 10 urban observation rainfall records. Additional WTs are identified that generate rainfall intensity between 100 and 150 mm/d, these being easterly wind, northerly wind and anticyclonic. The results of this study suggest that a WT-based correction is desirable.

A relatively simple and flexible cumulative probability distribution bias correction was applied that gives robust results within the methodology. By comparing the raw (i.e. not corrected) forecasts from the ECMWF, we show that cumulative 24, 48, 120 and 240 h lead-time forecasts show the underestimation of all WTs while highlighting strong

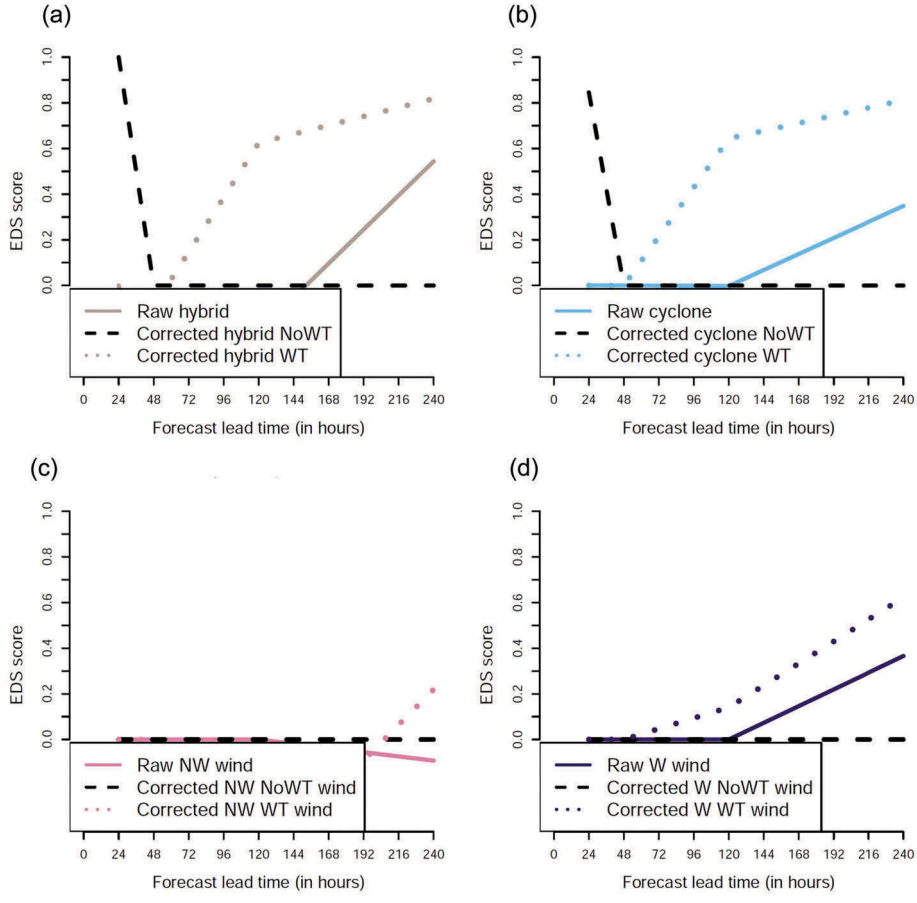

Figure 17. Extreme dependency plot per weather type for Tokyo station with a threshold of 100 mm/d. (a)–(d) Performance of individual hybrid, cyclone, NW and W wind WTs, respectively. The corrected global EDS (NoWT) is indicated by the dashed black line. The solid grey, blue, violet and pink solid lines indicated the observed EDS scores for the hybrid, cyclone, NE and W WTs. The coloured dotted lines highlight the performance of the specific WT bias correction for a rainfall threshold of 100 mm/d.

variations between them. We used 10 stations to investigate the statistical performance of the methods and show that bias correction reduces the root mean square error (RMSE) of the rainfall by about 0–10%, depending on the station, WT and forecast lead time. The WT classification bias-correction approach presents higher RMSE reduction than a global bias-correction method that does not use a WT approach in the majority of cases (90%). For the best cases, an additional 20% improvement could be observed due to the use of specific bias correction-based WT.

The EDS investigation showed that global bias correction (or NoWT) indicated good performance for rainfall events larger than 10 mm/d, but weak performance for events larger than 100 mm/d, except for 24 h lead time. The EDS score for events of >100 mm/d presented higher performance for WT-based bias correction for all lead times. The results obtained highlight the importance of WT-based bias correction for extreme rare events, and the limitations of a global bias-correction approach.

Finally, the analysis undertaken raises important questions for future research. First, in addition to the forecast lead time and weather type investigation, seasonality and the bias-correction method itself could be investigated. Second, similar methods should be extended to other urban areas and could help to highlight local geographical constraints which can determine the predominance of extreme rainfall associated WTs, as we saw at the Niigata station. A location close to the coastline or near mountains creates a local climate system, which differs from the regional pattern, as illustrated by Nagoya or Hamamatsu stations. Furthermore, the example of Niigata station suggests fewer occurrences of extreme rainfall but with a more diversified WT. Third, it would be interesting to investigate to what extent the results presented here advance the goal of improving dynamical downscaling using WT in a selection process for an operational flood alert system.

Acknowledgements

The authors thank the European Centre for Medium-Range Weather Forecasts (ECMWF), Reading, UK, for providing access to the TIGGE dataset and for the visit of Jean-Francois Vuillaume as a scientific guest during summer 2014. Souhail Boussetta (ECMWF), Singay Dorji (UNU-IAS) and B. Simon provided a useful review of the draft version of the paper, which contributed to the improvement of the paper.

Disclosure statement

No potential conflict of interest was reported by the authors.

ORCID

Jean-Francois Vuillaume http://orcid.org/0000-0002-8136-3481

References

Baltacı, H., *et al.*, 2015. Atmospheric circulation types in Marmara Region (NW Turkey) and their influence on precipitation. *International Journal of Climatology*, 35, 1810–1820. doi:10.1002/joc.4122

Bougeault, P., *et al.*, 2010. The THORPEX interactive grand global ensemble. *Bulletin of the American Meteorological Society*, 91, 1059–1072. doi:10.1175/2010BAMS2853.1

Bower, D., *et al.*, 2007. Development of a spatial synoptic classification scheme for western Europe. *International Journal of Climatology*, 27, 2017–2040. doi:10.1002/joc.1501

Calvo, A., *et al.*, 2012. Air masses and weather types: a useful tool for characterizing precipitation chemistry and wet deposition. *Aerosol and Air Quality Research*, 12, 856–878.

Coles, S., Heffernan, J., and Tawn, J., 1999. Dependence measures for extreme value analyses. *Extremes*, 2, 339–365. doi:10.1023/A:1009963131610

COST733, 2015. Harmonisation and applications of weather type classifications for European regions. *Online resource consulted the 4th April 2016*. Available from: http://cost733.geo.uni-augsburg.de/cost733wiki.

Dee, D., *et al.*, 2008. COST 733 – WG4: applications of weather type classifications. *Poster presented at COST 733 mid-term conference*, 22–25 October 2008 Krakow, Poland.

Demuzere, M., *et al.*, 2008. COST 733 – WG4: applications of weather type classifications. *In: COST 733 mid-term Conference*, Poster, 22–25 October 2008, Krakow.

Glahn, H.R. and Lowry, D.A., 1972. The use of model output statistics (MOS) in objective weather forecasting. *Journal of Applied Meteorology*, 11, 1203–1211.

Gneiting, T. and Katzfuss, M., 2014. Probabilistic forecasting. *Annual Review of Statistics and Its Application*, 1, 125–151. doi:10.1146/annurev-statistics-062713-085831.

Haiden, T., Janousek, M., and Richardson, D., 2014. Forecast performance 2014. *ECMWF newsletter*, Winter 2014/15, p. 4. Reading: ECMWF.

Hess, P. and Brezowsky, H., 1952. Berichte des Deutschen Wetterdienst in der US-Zone 33. *Katalog der Großwetterlagen Europas*, edited by DWT.

Husak, G., Michaelsen, J., and Funk, C., 2007. Use of the gamma distribution to represent monthly rainfall in Africa for drought monitoring applications. *International Journal of Climatology*, 27, 935–944. doi:10.1002/joc.1441

Huth, R., *et al.*, 2008. Classifications of atmospheric circulation patterns: recent advances and applications. *Annals of the New York Academy of Sciences*, 1146, 105–152. doi:10.1196/annals.1446.019

Jenkinson, A. and Collison, F., 1977. An initial climatology of gales over the North Sea. *Synoptic Climatology Branch Memorandum*, 62. Bracknell: UK Met. Office, 18 pp.

Jones, P., Hulme, M., and Briffa, K., 1993. A comparison of Lamb circulation types with an objective classification scheme. *International Journal of Climatology*, 13, 655–663. doi:10.1002/(ISSN)1097-0088

Katz, R., 1999. Extreme value theory for precipitation: sensitivity analysis for climate change. *Advances in Water Resources*, 23, 133–139. doi:10.1016/S0309-1708(99)00017-2

Kenawy, A.M., *et al.*, 2014. Multi-decadal classification of synoptic weather types, observed trends and links to rainfall characteristics over Saudi Arabia. *Frontiers in Environmental Science*, 2. doi:10.3389/fenvs.2014.00037

Lamb, H., 1972. British Isles Weather types and a register of daily sequence of circulation patterns, 1861-1971. *Geophysical Memoir* 116. London: HMSO.

Lee, C. and Sheridan, S., 2012. A six-step approach to developing future synoptic classifications based on GCM output. *International Journal of Climatology*, 32, 1792–1802. doi:10.1002/joc.v32.12

Philipp, A., *et al.*, 2010. Cost733cat - a database of weather and circulation type classifications. *Physics and Chemistry of the Earth*, 35, 360–373. doi:10.1016/j.pce.2009.12.010

Piani, C., Haerter, J., and Coppola, E., 2010. Statistical bias correction for daily precipitation in regional climate models over Europe. *Theoretical and Applied Climatology*, 99, 187–192. doi:10.1007/s00704-009-0134-9

Primo, C. and Ghelli, A., 2009. The affect of the base rate on the extreme dependency score. *Meteorology Applications*, 16, 533–535. doi:10.1002/met.152

Raftery, A., *et al.*, 2005. Using Bayesian model averaging to calibrate forecast ensembles. *Monthly Weather Review*, 133, 1155–1174. doi:10.1175/MWR2906.1

Riediger, U. and Gratzki, A., 2014. Future weather types and their influence on mean and extreme climate indices for precipitation and temperature in Central Europe. *Meteorologische Zeitschrift*, 23, 231–252. doi:10.1127/0941-2948/2014/0519

Rousi, E., *et al*., 2014. Classification of circulation types over Eastern Mediterranean using a self-organizing map approach. *Journal of Maps*, 10, 232–237. doi:10.1080/17445647.2013.862747

Shoji, T. and Kitaura, H., 2006. Statistical and geostatistical analysis of rainfall in central Japan. *Computers & Geosciences*, 32, 1007–1024. doi:10.1016/j.cageo.2004.12.012

Trigo, R. and DaCamara, C., 2000. Circulation weather types and their influence on the precipitation regime in Portugal. *International Journal of Climatology*, 20, 1559–1581. doi:10.1002/(ISSN)1097-0088

Verkade, J., *et al*., 2013. Post-processing ECMWF precipitation and temperature ensemble reforecasts for operational hydrologic forecasting at various spatial scales. *Journal of Hydrology*, 501, 73–91. doi:10.1016/j.jhydrol.2013.07.039

Wilks, D.S., 1995. *Statistical methods in the atmospheric sciences*. 2nd ed. International Geophysics Series, Vol. 59. New York: Academic Press, 467 p.